Coupled Oxidation of Heme Covalently Attached to Cytochrome b_{562} Yields a Novel Biliprotein†

Jane K. Rice,‡ Ian M. Fearnley,§ and Paul D. Barker*,||

Naval Research Laboratory, Code 6111, Washington, D.C. 20375-5342, and Laboratory of Molecular Biology and Centre for Protein Engineering, MRC Centre, Hills Road, Cambridge CB2 2QH, U.K.

Received April 14, 1999; Revised Manuscript Received October 4, 1999

ABSTRACT: A variant of *Escherichia coli* cytochrome b_{562} with covalently attached heme can be converted to a biliverdin-containing protein in two distinct stages by coupled oxidation and acid hydrolysis. The first stage of coupled oxidation yields a stable verdoheme-containing protein. This verdoheme protein is unusual in three respects. First, the verdoheme group is covalently bound to the protein through a *c*-type thioether linkage. Second, the oxidation stops at the verdoheme stage, and finally, this is the first report of verdoheme generated from a heme protein with exclusive methionine ligation to the heme iron. In addition, the oxidation process does not require denaturation of the protein. The product has been characterized by optical spectroscopy, ESI mass spectrometry, and ^{1}H NMR. The NMR data show that the predominant product is the result of oxidation at the α-meso carbon. A collective evaluation of data on the topic suggests that the electronic structure of the heme, not protein steric effects, is the main factor in controlling the regiospecificity of the oxidation site. In the second stage of conversion to a biliprotein, we demonstrate that the verdoheme ring can be opened by treatment with aqueous formic acid to give α-biliverdin covalently attached to the folded protein. This product, a protein-bound linear tetrapyrrole as characterized by optical spectroscopy and mass spectrometry, is an example of a phycobilin chromophore that has not been observed previously.

In the degradation of heme to biliverdin (Scheme 1),[1] the porphyrin is ring opened at the α-position by the enzyme heme oxygenase (HO-1 isoform found in liver and spleen, HO-2 isoform found in brain and testes) in the presence of molecular oxygen and electrons donated by cytochrome P450 reductase (*1*−*3*). The detailed structure of human HO-1 has only recently been determined (see Note Added in Proof). NMR studies of the heme environment have been reported (*4*). The electronic properties resemble those of cytochrome *c*′ type molecules.

One reported mechanism of the multiple oxidation steps is as follows. The HO enzyme first binds to the heme, forming an iron−histidine ligand similar to that of myoglobin and hemoglobin. The distal site of the heme is used to coordinate and activate O_2, leading to the regiospecific hydroxylation of the α-meso carbon of the heme that results in the hydroxyheme intermediate. The second step is the conversion of the α-mesohydroxyheme to verdoheme with the concomitant release of CO. In the final step, the verdoheme undergoes oxidative cleavage to form a biliverdin−iron complex that is released from the enzyme as ferrous iron and biliverdin. The α-mesohydroxyheme has not been directly observed as an intermediate in the normal catalytic process and therefore remains hypothetical. Alternatively,

Scheme 1

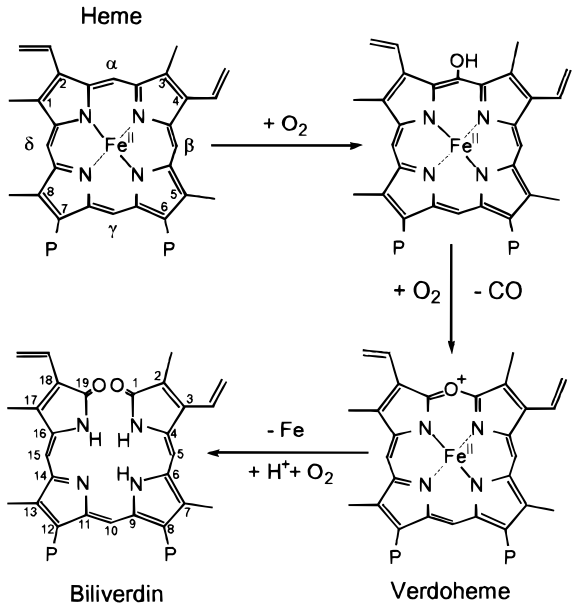

† This work was supported by the Office of Naval Research (ONR) through a travel grant (J.K.R.) and through the Naval Research Laboratory (J.K.R.), by the Biotechnology and Biological Sciences Research Council through an Advanced Fellowship (P.D.B.), and by the Medical Research Council through the Laboratory of Molecular Biology and the Centre for Protein Engineering.

* To whom correspondence should be addressed: Centre for Protein Engineering, MRC Centre, Hills Road, Cambridge CB2 2QH, U.K. Telephone: (+44-1223) 402130. Fax: (+44-1223) 402140. E-mail: pxb@mrc-lmb.cam.ac.uk.

‡ Naval Research Laboratory.

§ Laboratory of Molecular Biology, MRC Centre.

|| Centre for Protein Engineering, MRC Centre.

[1] The IUPAC numbering systems for heme and bilins do not give equivalent atoms the same number. In Scheme 1, heme is numbered according to the Fischer nomenclature (see ref *34* for discussion), while biliverdin is numbered according to the conventional bilin nomenclature (*35*).

10.1021/bi990880y
Published on Web 12/03/1999

oxidative degradation of iron protoporphyrin IX (in any oxidation or ligation state) catalyzed by HO-1 in the presence of peroxide does not require exogenous electrons and produces an enzyme-bound α-mesohydroxyheme intermediate that is stable (*5*).

The environment of the heme in cyanoferric heme oxygenase was studied using NMR by LaMar and co-workers (*6*). They concluded from a comparison of a heme with 2-fold symmetry to that of ferriprotoporphyrin IX that isomeric binding of the substrate iron porphyrin occurs in two orientations, each rotated 180° from the other around the $\alpha-\gamma$ meso axis. These occur in a ratio of about 1:1. The researchers were able to extend their conclusions to the non-cyanide-inhibited functional heme-bound heme oxygenase. They determined that the α-meso carbon is held in the same position in space relative to the protein environment in both isomers, which they concluded lead to consistent regiospecificity of the reaction toward the α-meso heme edge.

A highly bent structure of oxygen bound to the iron was suggested by Takahashi et al. (*7*) from the Raman stretching frequency of Fe−O−O. This angle was assigned a value of 110° and placed the distal oxygen within van der Waals distance of the α-meso edge carbon. It was suggested that the angle was the result of constraint by amino acid residues in the distal pocket. The mechanism of the first step, a ferric−hydroperoxide active oxygen intermediate to yield α-mesohydroxyheme, was first postulated to be either (1) a nucleophilic attack of iron-bound peroxide or (2) an electrophilic aromatic substitution (*8*). The latter mechanism is supported by the successful synthesis of α-mesoethoxyheme when ethylhydroperoxide was used in place of oxygen or peroxide (*9*). More recently, the electrophilic mechanism is suggested by the observation that electron-withdrawing and electron-donating substituents at the meso positions have opposite effects on the regiospecificity of the reaction (*10*, *11*).

A similar mechanism of heme degradation has also been proposed for the so-called coupled oxidation that occurs upon exposure of the globins and other heme-containing proteins to ascorbate under aerobic conditions. The coupled oxidation of protoheme IX pyridine hemochromogen in the absence of protein results in a mixture of the four possible biliverdin products (*2*) that result from oxidative attack at the four meso positions. Within a protein, the regiospecificity of this in vitro oxidation reaction is potentially variable, depending on the structure of each particular protein−heme complex. However, reaction in the myoglobin and hemoglobin active sites results in cleavage at the α-meso position exclusively (*12*−*15*). Similar specificity is also observed in the context of cytochrome b_5 (*16*). The recent work with HO-1 (*10*, *11*) and isolated heme (*17*) suggests that regiospecificity in these proteins is influenced principally by the distribution of electron density in the heme group. Therefore, there is still a question of how this is achieved given that the ligation states and structure of the heme pocket vary considerably among these different proteins.

Heme oxygenase production of biliverdin also occurs on the biosynthetic pathway of the phycobilin chromophores of the plant and algal biliproteins of the light-harvesting and photoreceptor complexes (*18*, *19*). In this pathway, biliverdin is reduced to (3*E*)-phytochromobilin, which is then attached to the apophycobiliprotein or apophytochrome protein through a single thioether linkage to a cysteine residue. This attachment is thought to be a spontaneous reaction between the ethylidine group at the 3-position of phytochromobilin (which is the spontaneous isomer of the vinyl group) and the protein thiol. The resulting thioether link is analogous to those found in *c*-type cytochromes, although the pyrrole ring becomes reduced across the 2,3 bond. Before the biosynthesis of these chromophores had been elucidated, Lagarias (*20*) attempted to convert covalently attached heme in mitochondrial cytochrome *c* to a phycobilin chromophore by coupled oxidation. Therefore, the resulting biliverdin group would have two thioether linkages to the protein. Subsequently, a variety of naturally occurring phycobiliproteins, some with two linkages to cysteine residues, has been identified. Many of these linear tetrapyrrole prosthetic groups have modifications to the basic biliverdin structure that result in differing photochemical properties and energetics (*18*, and references therein).

Cytochrome b_{562} from *Escherichia coli* and the cytochromes *c*′ from photosynthetic species belong to a class of cytochromes with a four-α-helix structural fold but no significant sequence similarity. Cytochromes c_{556} have undetermined structure but appear to have electronic properties similar to those of cytochrome b_{562} and are low-spin, six-coordinate cytochromes with fairly high redox potentials with methionine and histidine ligation. Cytochromes *c*′, unlike cytochromes b_{562} and c_{556}, have high-spin, five-coordinate heme centers with a histidine providing the only axial ligand. We have previously described a cytochrome b_{562} protein, R98C/H102M (*21*, *22*), which has heme covalently attached through a single thioether linkage between the cysteine 98 thiol and the 2-vinyl group. It also has bis-methionine coordination to the heme iron, although one of the methionine ligands is labile in the oxidized state and this protein has been shown to exist as a five-coordinate species (*21*). Therefore, there is a possibility that small ligands, including oxygen, could coordinate to the heme iron, although this has not previously been observed.

In studying a further variant of this R98C/H102M cytochrome b_{562}, containing a double amino acid deletion at the C-terminus, we have observed coupled oxidation of the heme that results in a biliverdin-containing protein in which the prosthetic group is covalently bound to the protein through a *c*-type thioether linkage. The oxidation is predominantly at the α-meso position, and the oxidation is arrested at the verdoheme stage. This is the first report of a protein-generated verdoheme from an iron not ligated to histidine. The effects of heme substituents on the electronic structure, the coordination of iron to the heme, the changes in the residues surrounding the heme, and the degree of exposure to solvent are all key issues in the following discussions. We also show that in a second stage of heme oxidation the verdoheme ring can be hydrolyzed to a linear tetrapyrrole that is a variant of the phycobilin chromophores not previously observed.

MATERIALS AND METHODS

Sodium ascorbate was obtained from Sigma. Potassium ferricyanide, sodium dithionite, and diethanolamine were Analar grade from BDH. All other materials were Analar grade or better, and water was either Elgastat or MilliQ

purified. All protein chromatography was carried out using a Waters model 625 liquid chromatograph equipped with a model 996 diode array detector. Absorption spectra in the visible region of the spectra were recorded on either a Hewlett-Packard 8453A diode array or a Cary 500 double-beam spectrometer. Absorption spectra were obtained in pH 4.5 or 5.0 (0.1 M acetate) or pH 8.5 (20 mM diethanolamine-HCl) buffers. SDS−PAGE was carried out on a Phastsystem (Pharmacia) using 20% acrylamide gels, followed by staining with Coomassie Blue or staining for heme (*23*). Kinetics of the verdoheme precursor oxidation were monitored in the visible spectral region following addition of ascorbic acid at either pH 5.0 or 8.5.

Cloning and Mutagenesis. The cloning and mutagenesis for obtaining the doubly mutated form (R98C/H102M) of cytochrome b_{562} has been described previously (*24*). The deletion of the codons for residues Y105 and R106 was carried out with a second set of PCR. The forward oligonucleotide, P1 (TCCGTACCATGGGACGTAAAAGCCTGTTAGCTATTCTTGCA), was the same as that used previously. It was designed to amplify the whole gene and contained the terminus for the engineered *Nco*I restriction site at the beginning of the b_{562} gene. The reverse oligonucleotide, P2 (ACGTCGGGATCCTTACTTCTGCATATAGGCGTTGCAGGTCGT), deletes the six base pairs corresponding to the codons for residues 105 and 106. It also contained the terminus for the engineered *Bam*HI restriction site at the end of the b_{562} gene. Vent polymerase (NEB) was used in the PCRs with annealing at 50 °C for 20 s and extension at 74 °C for 20 s for 25 cycles with a hot start. The DNA product was purified by agarose gel electrophoresis before digestion with both *Nco*I and *Bam*HI restriction endonucleases. The digested segment was religated into the purified 4.8 kb fragment of *Nco*I−*Bam*HI-cut plasmid, pCE820. The ligation mix was transformed into *E. coli* strain NM554 (Stratagene) by electroporation, and the recovered cells were plated onto TY agarose containing 0.1 mg/mL ampicillin and 0.1 mg/mL glucose. Clones expressing cytochrome b_{562} were identified by the orange cell color after overnight growth in 2× TY medium with 0.1 mg/mL ampicillin. The plasmid (pCEB562) was isolated from positive clones, and the sequence was confirmed using automated DNA sequencing methods.

Protein Expression, Purification, and Analysis. The protein expression method has been reported previously (*24*). The protein was obtained in the periplasmic extract containing 0.1 M Tris-HCl (pH 8.0), 10 mM EDTA, 20% sucrose, 0.1 mg/mL lysozyme, and 2 mM ascorbate. The heme was covalently attached to the protein in this periplasmic extract using the following procedure. The amount of apoprotein in the periplasmic extract was estimated by titration of a small fraction of undiluted extract with heme, monitored by optical spectroscopy in a cuvette with a 2 mm path length. Meanwhile, the bulk of the periplasmic extract was placed in a bottle, sealed with a septum, and made anaerobic by pumping out and flushing with oxygen free argon. Once the bottle was deemed anaerobic, the apoprotein was saturated with heme and the solution made 1 mM in D- or L-cysteine. The extract was then left for 48−60 h until the reaction was complete as judged by optical spectroscopy (P. D. Barker and E. P. Nerou, manuscript in preparation).

After the covalent linkage was made, the protein was partially purified by acid precipitation at pH 4.5. After centrifugation, the supernatant was concentrated and exchanged into 20 mM diethanolamine (pH 8.5) ready for anion exchange chromatography. The proteins were purified by chromatography on Q-Sepharose HP (Pharmacia, 30 mL of resin, self-packed) and then by gel filtration on Superdex 75 (XK26/60 Pharmacia) and finally polished by further anion exchange on Mono-Q columns (HR 5/5 and HR 10/10, Pharmacia). The verdoheme was noticed on the Q-Sepharose column the first time the protein was purified. First, a bright green protein eluted from the column followed by forest green protein. The bright green protein was later determined to be the protein covalently bound to the unusual verdoheme. In subsequent experiments, the periplasmic extract was left stirring in air overnight prior to separation to increase the yield of the verdoheme. The forest green material (later defined as the precursor) was also isolated, purified, and concentrated in the same manner. The yield of the precursor was maximized by limiting the exposure of ascorbate-containing solutions to air, thereby preventing the first reaction shown in Scheme 1. For this purpose, the periplasmic extract was concentrated and washed into non-ascorbate-containing buffers in a nitrogen atmosphere glovebox (Belle Technology). The parent protein (R98C/H102M) is purified as a single species (the reduced, heme-containing cytochrome) and as such is stable indefinitely.

The hydrolysis of the verdoheme prosthetic group was observed in time by optical spectroscopy and electrospray mass spectrometry. Samples, either aerobic or deaerated and placed under argon, of 10−100 mM verdoheme protein in water were taken to 8% (v/v) formic acid. The reaction was initiated by raising the temperature to 50 °C. Samples for mass spectrometric analysis were removed, placed on ice, and diluted 15- or 30-fold with an aqueous formic acid/acetonitrile mixture before introduction into the electrospray interface.

Mass Spectrometry. Mass spectrometry experiments were performed using a Sciex API III$^+$ mass spectrometer equipped with an electrospray ionization interface. The instrument was operated in positive ion mode, and both quadrupoles were tuned and calibrated using a mixture of poly(propylene glycol)s. The calibration was verified using horse heart myoglobin.

Protein samples were prepared for analysis by ultrafiltration into deionized water. Then immediately before analysis, they were diluted in 0.2−0.5% (v/v) formic acid in 50% aqueous acetonitrile to concentrations of about 5 μM. Samples were introduced into the ionization interface in a solvent comprising 50% aqueous acetonitrile at a flow rate of 3 μL/min, via a Rheodyne sample loop. A nanoelectrospray ionization source (*25*) was used for all tandem ms[2] experiments and some measurements of molecular mass. The protein ions produced by electrospray ionization were analyzed in quadrupole Q1 by scanning between m/z 600 and 1800 in 12.6 s, with a step size of 0.1 Da and a dwell time of 1 ms. For tandem ms experiments, intact protein ions, carrying 10, 11, or 12 positive charges, were selected from the mixture of protein ions (carrying different numbers of charges) and fragmented by collision with argon in the

[2] Abbreviation: ms, mass spectrometry.

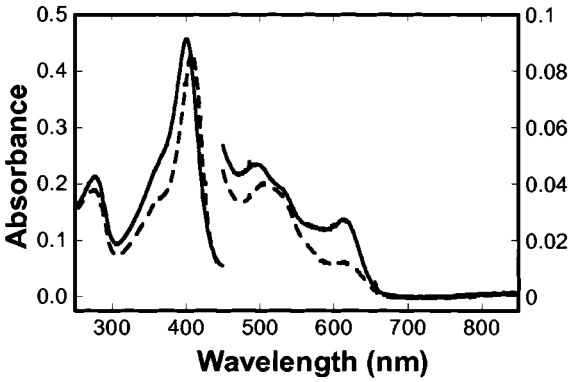

FIGURE 1: Optical spectrum of ferric, heme-containing Δ105,106 R98C/H102M cytochrome b_{562} at pH 8.5 (solid line) and 4.5 (dashed line). The protein concentration is approximately 5 μM.

collision cell (Q2). The fragment ions were recorded by scanning the third quadrupole across *m*/*z* 300−1200. Preferential cleavage of the thioether linkage of the heme rather than scission of the polypeptide chain occurred with a voltage drop of 20−30 V across the collision cell and a partial pressure of argon, recorded as collision gas thickness, of 2.6 $\times$ 10^{14} molecules/cm^2.

NMR Spectroscopy. Verdoheme-containing protein samples were prepared for ^{1}H NMR by concentrating and exchanging into D_2O-containing buffer [0.1 M phosphate and 0.5 M KCl (pH* 6.6)] for deuterium exchange of the amide protons. Estimated concentrations are ∼2 mM. The other proteins described below have not been purified in sufficient quantities for analysis by NMR. Spectra were recorded at 300 K using a Bruker AMX 500 spectrometer with an operating frequency of 500.13 MHz. ^{1}H homonuclear two-dimensional NOESY and clean-TOCSY experiments were performed as previously described (*24*) and acquired as two-dimensional matrices of 2048 $\times$ 256 complex points with 64 or 128 transients per increment. The sweep width in all experiments was set to 10 204 Hz. Data were processed (by 2-fold zero filling and apodization with a 45°-shifted sine-bell window function) and analyzed using FELIX 97 (MSI).

RESULTS

Formation and Characterization of the Verdoheme Protein. When the cytochrome b_{562} mutant R98C/H102M is expressed and the heme attached in vitro as described in Materials and Methods, the orange-pink reduced protein can be purified in air without problems and is identical to that previously described (*21*). We will refer to this protein as the parent protein. The first attempt to purify the protein with the C-terminal deletion, Δ105,106 R98C/H102M, resulted in predominantly green proteins. The bright green verdoheme-containing protein eluted first from anion exchange columns, while a darker, forest green fraction eluted later. This latter material, shown below to contain a heme prosthetic group, gives electronic spectra similar to those of the parent protein. In the ferrous state, this protein has an optical spectrum identical to that of the parent protein at all pH values (data not shown). The deletion mutant is, however, different in one important respect. The optical spectrum of the ferric protein (Figure 1) reveals that the protein is predominantly high-spin at all pH values, as judged by the presence of the 630 nm absorption band. This suggests that

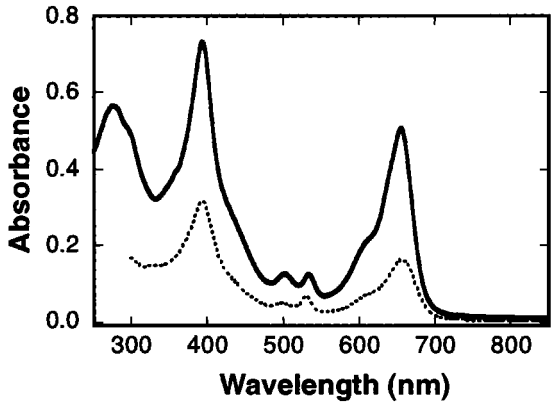

FIGURE 2: Optical spectra of verdoheme-containing Δ105,106 R98C/H102M cytochrome b_{562} at pH 7.0 (solid line) and of the pyridine hemochrome (dotted line) from the same protein. Protein concentrations are approximately 18 and 6 μM, respectively. The presence of 25% pyridine precludes measurement below 300 nm in the latter spectrum.

Table 1: Comparison of Visible Absorption Bands of Various Isomers of Pyridine−Verdohemochrome IX with the Cytochrome b_{562} Protein-Bound Pyridine-Verdoheme (Indicated as X)

isomer	absorption maxima (nm) (relative peak intensity)			
Py_2-X[a]	393 (1.0)	498 (0.16)	531 (0.22)	657 (0.54)
Py_2-α[b]	398 (1.0)	504 (0.18)	535 (0.23)	680 (0.67)
Py_2-β[b]	397 (1.0)	502 (0.16)	533 (0.25)	669 (0.64)
Py_2-γ[b]	396 (1.0)	495 (0.21)	530 (0.30)	654 (0.62)
Py_2-δ[b]	397 (1.0)	500 (0.16)	534 (0.22)	664 (0.76)

[a] This work. [b] From ref *2*.

the low-spin, bis-methionine coordinated species observed at low pH in the parent protein has been destabilized and that this new protein may be five-coordinate at all pH values. High-resolution anion exchange chromatography revealed that the ferric material could be partially resolved into two species. These species had identical visible spectra and also identical molecular masses (within 1 Da, data not shown). As shown below, this forest green fraction is the precursor to the verdoheme-containing protein. All the proteins isolated here stained positively with tetramethylbenzidine in the peroxidase assay following denaturing SDS gel electrophoresis (*23*), thus providing initial evidence that all these proteins have a covalently bound prosthetic group.

The protein-bound verdoheme in the bright green fraction was identified by several methods. The optical spectrum of the protein is characteristic of verdoheme-containing systems. This spectrum and that of the pyridine hemochrome (*26*, *27*) of this bright green species are shown in Figure 2. The absorption maxima of our pyridine−verdoheme−protein complex together with those of the four pyridine−verdohemochrome IX isomer forms (*28*) are given in Table 1. Although the absorption maxima and their intensity ratios do not match those of any of the four verdoheme isomers, they are closest to those of the γ-isomer. The loss of a vinyl group due to the covalent attachment is expected to shift the spectra to lower wavelengths, but only the Soret band appears at a wavelength lower than observed from any of the four isomers.

The heme proteins were characterized by electrospray mass spectrometry performed on protein samples denatured by dilution into solutions containing acidic 50% aqueous acetonitrile. The molecular mass of the forest green precursor

Table 2: Molecular Masses of the Mutant Cytochrome b_{562} Proteins Measured by ESI MS under Acidic, Denaturing Conditions

protein	molecular mass (Da) (SD) measured	expected[a]
R98C/H102M (parent)[b]	12 337 (1.1)	12 338
Δ105,106 R98C/H102M heme-containing (precursor)	12 018 (1.3) 12 017 (0.66)	12 018
Δ105,106 R98C/H102M verdoheme-containing	12 019 (0.37) 12 020 (1.3)	12 021

[a] Mass of polypeptide plus heme or verdoheme. [b] From ref *21* and this work.

protein was determined to be 12017−12018 Da, while the verdoheme protein gave masses of 12019−12020 Da (Table 2, multiple measurements were obtained from each sample, and the results are within the 0.01% mass accuracy of the instrument). The theoretical mass difference between the verdoheme and its precursor is 3 Da. To confirm the mass of the prosthetic group and confirm that the observed differences arose from prosthetic group modification rather than apoprotein modification, the proteins were analyzed by tandem mass spectrometry. In these experiments, the covalently attached heme was dissociated from protein ions by collision-induced dissociation with argon in the collision cell (Q2) of the mass spectrometer and the resultant heme ions assessed using Q3. Portions of the fragment ion spectra for the parent, precursor, and verdoheme proteins are shown in Figure 3. These spectra were generated by the selection and fragmentation of protein ions carrying 11 positive charges, though identical spectra were obtained by dissociation of molecular ions carrying either 10 or 12 charges. Fragment ions at *m*/*z* 616 and 617 (Figure 3a,b) were obtained from tandem ms of ions from the parent and precursor proteins, whereas fragment ions at *m*/*z* 619 and 620 (Figure 3c) were obtained from the same tandem ms experiments performed on the verdoheme protein. As expected, the abundance of heme fragment ions relative to intact protein ion could be altered by adjustments to the collision energies in the mass spectrometer. The difference in mass of 3 Da confirms the identity of the verdoheme species.

The two main ions observed are not due to the isotope distribution, but rather to ferric and ferrous oxidation states of the heme fragments (*29*). In panels a and b of Figure 3, the ions at *m*/*z* 616 correspond to the oxidized state, which carry a single charge due to the ferric heme ion. With the propionates protonated, the ferrous heme ion has no net charge, and so for the ferrous fragment to be observed, it must be protonated further, hence the extra 1 Da in mass. This would also explain the presence of the ions at *m*/*z* 619 and 620 in Figure 3c. No doubly charged heme ions were observed in any spectra. The same distribution of heme fragment ions was observed when protein samples were ionized under neutral (native) conditions from a solution of 10 mM ammonium acetate at pH 6.8, although the intensity of fragment ions was much lower. A similar pattern of heme fragment ions was obtained by tandem ms of horse heart cytochrome *c* when ionized from denaturing solutions containing acidic acetonitrile (not shown). This same distribution of heme ions has been noted previously from fragmentation of cytochrome *c* ions by "in source" fragmentation rather than by collision-induced dissociation (*29*).

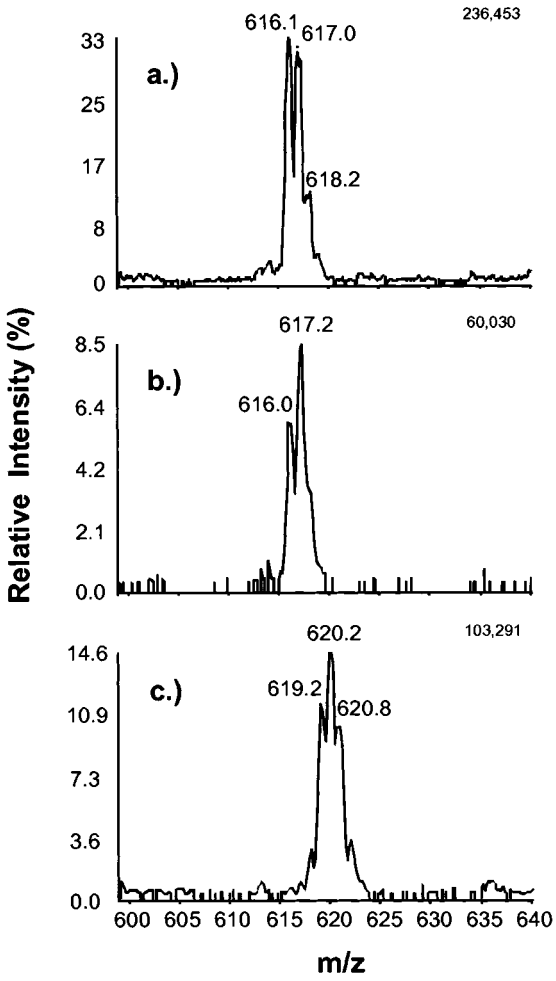

FIGURE 3: Portions of the tandem mass spectra of (a) R98C/H102M cytochrome b_{562}, (b) heme-containing Δ105,106 R98C/H102M cytochrome b_{562}, and (c) verdoheme-containing Δ105,106 R98C/H102M cytochrome b_{562}.

The ferric, heme-containing precursor protein was incubated at 40 °C in the presence of 1 mM ascorbate at pH 5 or 8.5. The resulting optical changes were recorded as either absolute or difference spectra (in which the initial oxidized spectrum is subtracted from subsequent data). An example is shown in Figure 4. The formation of verdoheme is rapid, compared with coupled oxidation in other proteins (*15*, *16*, *30*), and is essentially complete within 4 h at either pH value. The verdoheme absorbance at 656 nm appears in a manner close to first-order with a rate constant of 10^{-3} s^{-1}. The changes in absorbance in the Soret region are more complicated and reveal that the overall process is not first-order. Clearly, some reduced heme protein can be observed initially, but the verdoheme is the only other spectral species that can be readily identified.

Conversion of the Verdoheme to a Biliverdin. When the verdoheme-containing protein was incubated with 8% formic acid at 50 °C under air or argon (*20*), the characteristic blue color of a biliverdin-type chromophore was observed. The rate of reaction was dependent on the degree of exposure to air. In air, the reaction was complete within 3 h. Stringent removal of air from the samples rendered the verdoheme essentially stable to further oxidation. The changes in the optical spectrum observed during the first 180 min of the

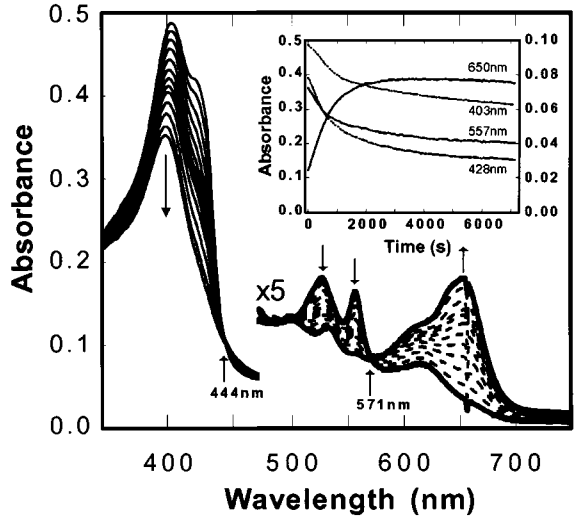

FIGURE 4: Time course of the coupled oxidation of the heme-containing Δ105,106 R98C/H102M cytochrome b_{562}. Spectra were recorded 1, 3, 5, 7, 9, 11, 13, 15, 17, 21, 31, 60, and 120 min after addition of ascorbate to the protein solution (~5 μM) at pH 8.5 and 40 °C. The arrows indicate the direction of change at that wavelength, and the labeled arrows indicate isosbestic points. The spike at 656 nm is a spectrophotometer artifact. The inset shows the kinetics of the reaction at four different wavelengths. The left-hand absorbance scale refers to the 403 and 428 nm traces, while the right-hand axis refers to the 557 and 650 nm traces.

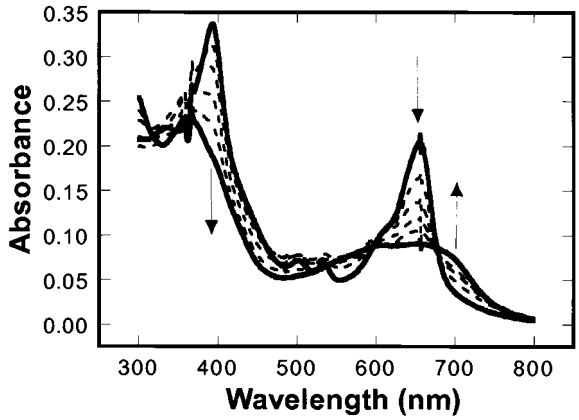

FIGURE 5: Time course of the spectral changes following treatment of verdoheme-containing Δ105,106 R98C/H102M cytochrome b_{562} with 8% formic acid in an aerobic, aqueous solution at 50 °C. Spectra were recorded 0, 10, 30, 60, 120, and 180 min after addition of formic acid. The arrows indicate the direction of change at that wavelength.

incubation in air are shown in Figure 5. No further changes were observed after a further 4 h. The hydrolysis was also monitored by mass spectrometry. Protein mass spectra at four time points after initiation of the hydrolysis are shown in Figure 6. The mass of the starting material is consistent with the verdoheme-containing protein described above. Initially, two new species appear, with masses of 12 036 and 11 985 Da. The 11 985 Da component soon becomes the major species that is observed. The 12 036 Da intermediate species has a mass that is 16 ± 1 Da higher than that of the starting verdoheme protein, consistent with the addition of one oxygen atom to the molecule. The final product (11 985 Da) has a mass that is 35 ± 1 Da lower than that of the verdoheme protein (12 020 Da) and 51 ± 1 Da lower than that of the intermediate species, which is consistent with the loss of iron and the gain of four to five protons. A fourth,

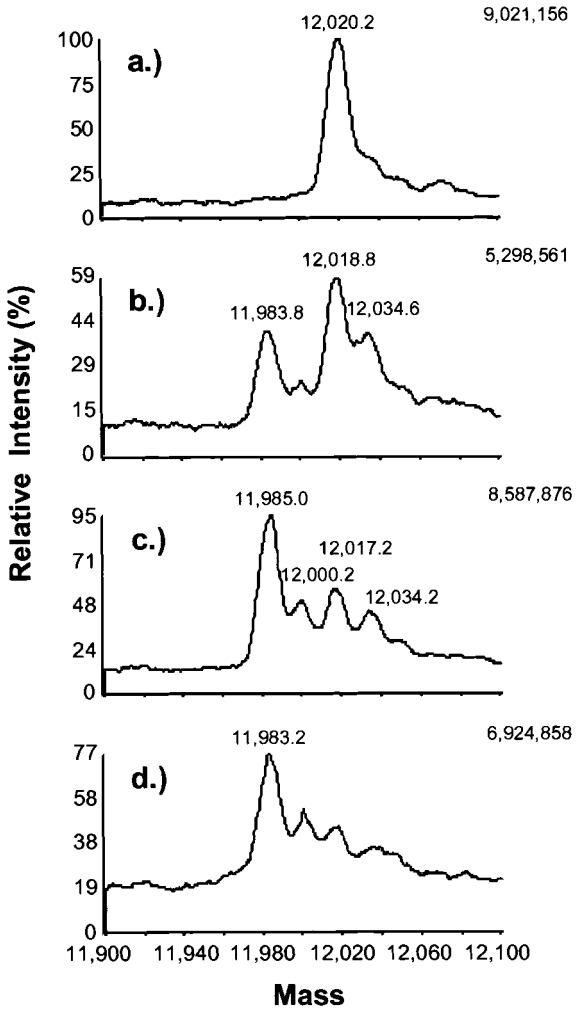

FIGURE 6: Time course of the hydrolysis of verdoheme-containing Δ105,106 R98C/H102M cytochrome b_{562} with 8% formic acid in aqueous solution at 50 °C as followed by electrospray mass spectrometry. The spectra have been simplified by mathematical reconstruction of the envelope of multiply charged species from raw data at different *m*/*z* ratios onto a true mass scale. Samples were analyzed at (a) 0, (b) 60, (c) 180, and (d) 1140 min.

minor component (12 000 Da) is also observed with a mass that is 15 ± 1 Da higher than that of the final product. Once again, the mass of the protein-bound prosthetic groups in each of these species cannot be determined to better than ±1 Da by analysis of the intact protein. Therefore, tandem ms experiments were performed to determine the mass of the prosthetic group covalently attached to the protein. Fragmentation of either the 11+ or 12+ ion (at *m*/*z* 1090.6 and 999.8) from the 11 985 Da species gave one singly charged fragment with a mass of 583 Da. This mass is consistent with the chromophore being biliverdin attached to the protein. Since the calculated apoprotein mass is 11 402 Da, these measurements confirm that no modifications to the polypeptide occur during the hydrolysis of the verdoheme.

After lyophilization and buffer exchange, the hydrolyzed verdoheme protein was subsequently chromatographed by ion exchange chromatography and gel filtration. The far-UV CD spectrum (not shown) of this biliprotein was very similar to that of the parent protein and characteristic of the four-helix bundle. This showed that the protein is still folded after hydrolysis of the verdoheme. The new chromophore

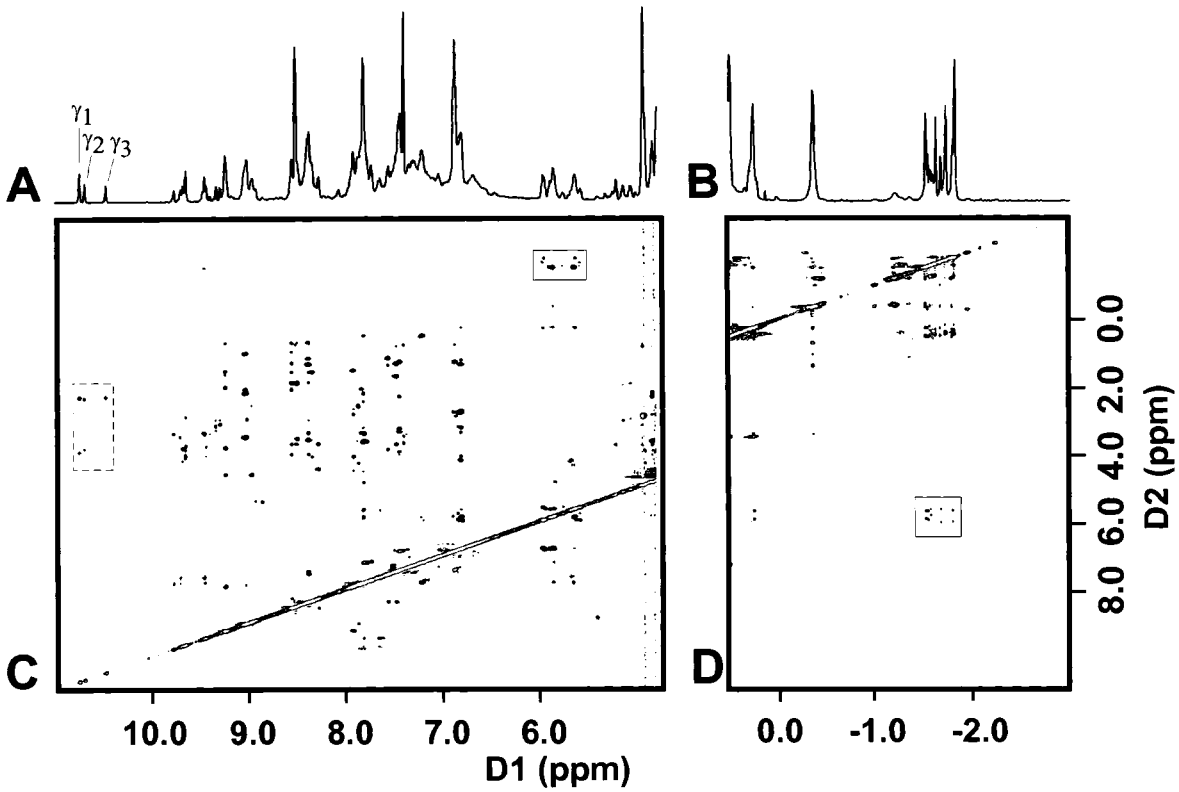

FIGURE 7: ^{1}H NMR spectra of verdoheme-containing Δ105,106 R98C/H102M cytochrome b_{562}. Low-field (A and C) and high-field (B and D) sections of one-dimensional (A and B) and NOESY (C and D) spectra. For conditions, see the text. Cross-peaks between the Met7 and Phe65 protons are enclosed in solid lines. The main cross-peaks involving the γ-meso proton resonances are enclosed in dashed lines.

does not fluoresce significantly in either the folded or unfolded protein. The optical spectrum of the protein in a 10 mM trifluoroacetic acid solution has two maxima at 370 and 660 nm with an absorbance ratio of 2.2:1.

Identification of the Site of Oxidation by NMR Analysis. The verdoheme-containing cytochrome b_{562} was the only protein described here that we have analyzed by NMR. Surprisingly, the ^{1}H NMR spectra of this protein are more complex than expected, revealing that the protein is heterogeneous with several very closely related species being present. Qualitatively, the spectra are similar to that of the parent protein in the ferrous state (*22*), confirming that the verdoheme contains diamagnetic, low-spin iron(II). Portions of the ^{1}H one-dimensional spectrum of the verdoheme-containing protein are shown in panels A and B of Figure 7. The downfield region of the NOESY spectrum is shown in Figure 7C, and the upfield region is shown in Figure 7D. The ring current-shifted methionine ligand resonances are obvious at high field (−1 to −2 ppm), although nine signals can be assigned to the ε-methyl resonance of ligand residues 7 and 102. On the basis of NOEs observed to Phe65 protons (enclosed in panels C and D of Figure 7) (*22*), six of these signals are assigned to the ε-CH_3 of Met7, while three are assigned to those of Met102.

There is also heterogeneity in the heme proton signals, and three main sets of heme signals can be identified. The strongly deshielded meso protons are observed, as usual for diamagnetic heme systems, between 11 and 9 ppm. Three signals from each of three meso protons can be identified by their cross-peak patterns in the NOESY spectrum (Figure 7C), as highlighted for the γ-meso proton that gives rise to resonances $\gamma_1-\gamma_3$. Assignment of the heme protons proceeded as described previously (*22*), and their chemical shifts in the three main species (**1**−**3**) are given in Table 3. These species account for around 80−90% of the total integrated area of isolated heme proton resonances in an approximate ratio of 2:1:1 (e.g., resonances $\gamma_1-\gamma_3$ in Figure 7A). The patterns of cross-peaks for the three signals assigned to one particular meso proton are very similar despite differences in their chemical shifts (Table 3). Thus, the same three meso protons are present in each of the main heme species observed in the spectrum, and we conclude that the site of oxidation (where oxygen replaces the meso carbon and hydrogen atoms) is the same in these three species.

Table 3: Chemical Shifts[a] of Heme Resonances in Verdoheme-Containing Δ105,106 R98C/H102M Cytochrome b_{562}

heme group[b]	species **1**	species **2**	species **3**
1-methyl (21)	4.03	3.81/4.19	4.02
2-methine (31)	5.14	5.06	4.94
2-methyl (3^2)	1.97	1.92	1.96
α-meso (5)	*c*	*c*	*c*
3-methyl (7^1)	1.56	*d*	*d*
4α-vinyl (8^1)	7.64	7.66	7.84
cis-4β-vinyl (8^2)	5.67	5.69	5.65
trans-4β-vinyl (8^2)	4.20	4.23	4.34
β-meso (10)	9.46	9.71	9.77
5-methyl (12^1)	3.38	3.48	3.40
γ-meso (15)	10.75	10.70	10.48
8-methyl (18^1)	4.10	4.19/3.81	3.75
δ-meso (20)	9.65	9.68	9.43

[a] Parts per million vs DSS; from spectra obtained in 0.1 M phosphate and 0.5 M KCl at pH* 6.6 and 300 K. [b] Heme substituents are numbered according to the Fischer notation of the carbon atoms, with the IUPAC numbering given in parentheses. [c] Not present in this protein. [d] Unassigned.

The meso proton resonances were assigned to β-, δ-, and γ-meso protons on the basis of self-consistent NOEs observed to other heme protons and also NOEs observed to the methionine ligand protons. This latter evidence assumes that there has been no major rearrangement, upon heme oxidation, of either the heme in the protein or the ligand residues. The similarity in the overall pattern of NOEs to that in the parent protein (*22*) suggests that this assumption is valid. Key evidence which shows that there is no proton at the α-meso position in any of the three main species is the absence of an NOE between the 2-C$\underline{H}$ or 2-C$\underline{H}_3$ protons and any proton in the meso region (8−11 ppm). The 2-position substituents were identified by strong cross-peaks between the 2-C$\underline{H}$ protons and the 2-C$\underline{H}_3$ protons in the TOCSY and by the NOEs observed between the 2-C$\underline{H}_3$ protons and the 1-C$\underline{H}_3$ protons (data not shown).

DISCUSSION

We have identified a variant of cytochrome b_{562} in which the covalently attached heme can be selectively oxidized at the α-meso carbon in two distinct steps to yield a biliprotein. This oxidation of heme after its attachment to the protein contrasts with the biosynthesis of biliproteins in plants and algae, in which "free" heme is converted to modified biliverdins prior to their attachment to the polypeptide. Our biliprotein, however, is essentially photochemically inert, having very low quantum yields, presumably due either to efficient radiationless de-excitation pathways as observed for the linear tetrapyrroles free in solution or to strong quenching by the protein.

First-Stage Oxidation to Verdoheme and the Site of Oxidation. After the first stage of coupled oxidation, which occurs primarily during isolation, the Δ105,106 R98C/H102M cytochrome b_{562} variant is obtained with a stable verdoheme prosthetic group covalently attached to the protein. Evidence which shows that the oxidation has occurred at the α-meso carbon is provided by the NMR analysis of the major verdoheme species. We presume that the pyridine hemochrome spectrum is blue shifted relative to that of free α-verdoheme due to the covalent linkage and loss of the vinyl group. The three main species identified by NMR spectroscopy have the same protein mass, to within 1 Da. In addition, the results of tandem mass spectrometry show that the verdoheme groups in these species have identical masses. The heterogeneity could result from conformational and/or stereochemical differences around the heme site. The methionine ligands can theoretically adopt *R* or *S* conformations, at the sulfur atom, which would not readily interconvert without dissociation from the iron. There is also the possibility that the covalent attachment of heme to the protein in the in vitro reaction resulted in both stereochemistries at the 2-carbon atom of the heme. This is definitely not the case for the parent protein (R98C/H102M cytochrome b_{562}), but we cannot preclude this possibility for the deletion mutant, which may bind heme with a lower affinity in the first instance. The NMR data are inconclusive in this respect since there is no α-meso proton to help orient the 2-position substituents. In addition, cross-peaks involving these 2-position substituent protons are not distinguishable in the crowded aliphatic region of the NOESY spectrum.

It is quite surprising that the oxidation proceeds at the α-meso carbon. If we were to assume a mechanism involving the replacement of the most exposed meso carbon, examination of the structure of cytochrome b_{562} suggests oxidation should occur at the γ-carbon, which is expected to be most exposed when C-terminal residues 105 and 106 are removed. In addition, the charge distribution of the protein with or without residues 105 and 106 indicates an overall negative charge in the region of the γ-meso carbon that could stabilize the oxycation of verdoheme. Since we do not see involvement of the γ-meso carbon, we may assume a mechanism involving tilted oxygen binding to iron and reaction at the most electron-rich meso carbon, as seen in the case of HO-1 (*10*, *11*). For HO-1, it was originally proposed that the five-coordinate character and the influence of the distal pocket opposite the oxygen binding site were crucial to the regiospecificity of the reaction (*5*, *10*). However, there are unlikely to be any fortuitously positioned side chains to fulfill any such role in our cytochrome b_{562} protein.

It has since been suggested (*10*, *11*) that for HO-1, the electronic structure of the heme is the most important influence on the reactive site. The effects of electronic structure of the heme upon the regiospecifity of the reaction in the absence of protein have also been studied (*17*). Upon introduction of the electron-withdrawing CF_3 group at different positions in heme, it was shown that the most electron-rich carbon was the site of coupled oxidation. The strongest influences on the electron density in the heme are the type and position of ring substituents and ligands. The engineered covalent linkage in our parent protein and verdoheme results from the conversion of a vinyl group at position 2 to a thioether group. The SR group is more electron-withdrawing than the $CH{=}CR_2$, group but the CH_3 is generally electron-donating; therefore, the overall effect of the substitution with $CH(CH_3)SR$ is not expected to significantly alter the electronic structure. On the basis of electron density calculations in isolated heme (*17*), the propionates appear to be more electron-withdrawing groups than vinyl or ethyl groups. This factor steers the reactive site to the α-meso carbon position. Thus current analysis supports the electrophillic attack at the most electron-rich meso carbon as being the predominant mechanism in both the natural enzyme and the nonenzymatic systems.

Coupled oxidation of free hemin results in a 3:2 bias toward oxidation at the α-meso position over the other meso carbons. But within several, unrelated protein environments, coupled oxidation of heme at the α-meso position accounts for 90−100% of the product. Therefore, electronic effects due to differences in either the ligation or protein nearest neighbors are expected to account for the additional bias. Since the cytochrome b_{562} protein scaffold bears no relation in sequence or structure to that of myoglobin, cytochrome b_5, or (presumably) HO-1, we may assume that the protein nearest neighbors are less important and the ligation geometry is most important. It is interesting to note, however, that the presence of methionine ligands in cytochrome b_{562} does not alter the regiospecificity.

Recent literature reports (*10*, *11*, *17*) together with the data presented here lead to a shift away from the view that the distal pocket strongly influences regiospecificity and instead have placed the influence of electronic structure due to substituents of the heme and ligands to the iron above other factors. As stated above, the five-coordinate character of the iron group appears to be a prerequisite for the formation of

the verdoheme intermediate and subsequent products. Although the parent cytochrome b_{562} species has six-coordinate character at low pH and five-coordinate character at high pH, a verdoheme-containing product has never been observed from that mutant. The optical spectra (Figure 1) suggest that the Δ105,106 mutant has five-coordinate character throughout the pH range of 5−8.5 and allows the coupled oxidation to proceed at either pH 5 or 8.5. While trace amounts of verdoheme-containing species have been observed during purification of the wild type and a large variety of variant cytochrome b_{562} proteins, none of these mutants have formed verdoheme-containing proteins at any significant rate or in any significant quantity. We have established previously by NMR spectroscopy (*22*) that the parent R98C/H102M cytochrome b_{562} is Met-Met, six-coordinate in the ferrous state. In the ferric state, results from magnetic circular dichroism (*21*) showed that the protein exists in a pH-dependent equilibrium between low- and high-spin species, which are six- and five-coordinate species, respectively. The protein described here, Δ105,106 R98C/H102M cytochrome b_{562}, is the only one of many variants (J. K. Rice and P. D. Barker, unpublished results) that we have constructed that exists as a high-spin system in the ferric state at all pH values (Figure 1). The propensity to form a five-coordinate state may be the most important factor in determining the propensity for coupled oxidation in the cytochrome b_{562} context. It does not appear that any resulting increase in solvent exposure due to the deletion has any consequence for heme oxidation.

Our protein system for heme oxidation is the first to be described that does not have a histidine involved as a ligand. As described above, the five-coordinate state of these cytochrome b_{562} variants has a methionine as the only axial ligand. We have not identified which methionine is the labile one, although we have some evidence that either can dissociate from the iron depending on the sequence context (P. D. Barker, unpublished results). The lack of a nitrogen-containing ligand has been reported only once in an isolated heme environment, with the recent report of the conversion of octaethylporphyrin to verdoheme in the presence of a cyanide ligand (*31*).

Why does the reaction stop at the verdoheme stage? A stable verdoheme product has also been reported in an H63M variant of cytochrome b_5 protein (*16*, *30*). The addition of ascorbate to this cytochrome b_5 variant allows efficient coupled oxidation of heme that stops at the verdoheme stage, similar to that observed here. That system contains a six-coordinate iron with histidine and methionine axial ligands in the ferrous state, but the authors speculate that one ligand is replaced for the coupled oxidation to occur (*16*). Indeed, further studies indicate that a high-spin ferric species exists with histidine 39 and water as the two axial ligands (*30*). They suggest that the verdoheme product is the final one because of the stabilization of the ferrous, six-coordinate state by the ligation of methionine 63, as indicated by the inability of CO to displace a ligand (*30*). In our system, the two sulfur−iron bonds must further stabilize the ferrous heme state and strongly favor the arrest of the coupled oxidation at the verdoheme stage. It will be interesting to measure the redox potential of the verdoheme cytochrome b_{562}, given that the bis-methionine coordinated heme-containing cytochromes b_{562} are some of the highest-potential cytochromes known

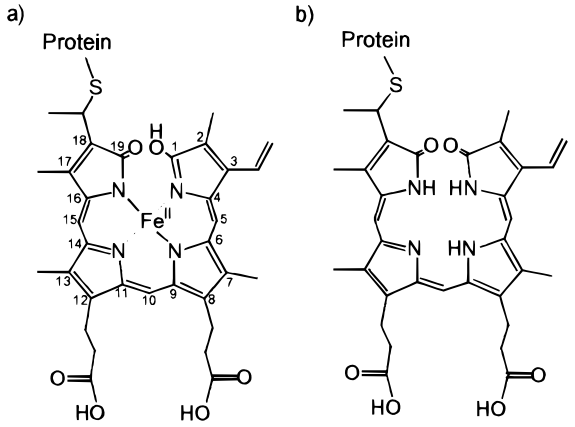

FIGURE 8: Predicted structures of the populated intermediate and main product of hydrolysis of the verdoheme prosthetic group. (a) Iron biliverdin, the species with a mass of 12 035 Da observed in Figure 6. (b) Cys-18′ biliverdin, the final product with a mass of 11 985 Da observed in Figure 6.

(ref *21* and unpublished results).

Second-Stage Oxidation to a Biliverdin. Treatment of the verdoheme protein with formic acid yields a protein with a covalently attached biliverdin, as shown by mass spectrometry and optical spectroscopy. Initial results suggest that dioxygen is required for this ring-opening step, but that exogenous reductants are not. During the hydrolysis, an intermediate is observed. It has a mass consistent with a structure (Figure 8a) in which the verdoheme ring is oxidatively opened and a second oxygen added but with the iron still coordinated. The mass difference between the intermediate and the stable product, which remains after hydrolysis, is consistent with the loss of iron and protonation of the pyrrole nitrogens. Given the chemical structure of the parent heme protein and the site of heme oxidation in the verdoheme protein, the stable prosthetic group must be α-biliverdin, attached at the 18-position to the cysteinyl residue of the protein (Figure 8b). Using the semisystematic nomenclature of Beale (*18*), this biliverdin group should be described as 8,12-bis(2-carboxyethyl)-18-[1-(cysteinyl-*S*-)-ethyl]-2,7,13,17-tetramethyl-3-vinylbilin-1,19(21*H*,22*H*,24*H*)-dione. The phycobilin that most resembles this chromophore is the Cys-mesobiliverdin from the Crytophycean phycocyanin 645 (*32*) in which mesobiliverdin is attached to the polypeptide at the 3′-position rather than at the 18′-position in our chromophore. When the proteins are denatured in 10 mM trifluoroacetic acid, the optical spectra of these two chromophores are qualitatively very similar.

The cytochrome b_{562} protein that results from the two stages of oxidation could be described as a new biliprotein. Whereas the biliproteins are assembled from modified biliverdin derivatives after heme oxidation, our protein has heme attached to the protein prior to heme oxidation. The biliverdin described here does not fluoresce in the folded protein at pH 7.0 (data not shown). The similarity of the peptide CD spectrum of the biliverdin-containing protein with that of the parent protein suggests that the four-helix bundle remains intact. The biliverdin is most likely, therefore, to remain in its closed, cyclohelical conformation, retaining the close packing with the polypeptide that existed between heme and the parent four-helix bundle and as seen in the biliverdin−myoglobin complex (*33*). Since the covalent linkage can be engineered into cytochrome b_{562} and the coupled

oxidation is facile, it may be possible to synthesize a variety of protein-bound linear tetrapyrrole structures that vary in the position of covalent attachment to the protein. Conditions may then be found in which the chromophore exists in the extended, linear conformation observed in the photoactive forms of the phycobiliproteins and phytochromes. The exact conformation of the linear tetrapyrrole in the cytochrome b_{562} protein remains to be determined.

CONCLUSIONS

We have carried out coupled oxidation of heme in a new protein environment to form covalently linked verdoheme. We have shown that the histidine ligand or any nitrogen-bonding ligand is not necessary for the conversion of heme to verdoheme. In this new protein and ligand environment, α-meso regiospecificity of coupled oxidation to form verdoheme is observed. We concur with previous studies that five-coordinate heme facilitates coupled oxidation reactions. We have also provided support for the view that within a protein environment, the regiospecificity of coupled oxidation is most strongly influenced by electronic factors. We have been able to chemically open the porphyrin ring to form a covalently linked α-biliverdin that is a phycobilin chromophore not previously observed in the phycobiliproteins. With our ability to manipulate the point of covalent attachment, the possibility exists for engineering new photoreceptors containing unnatural linear tetrapyrroles.

NOTE ADDED IN PROOF

Schuller et al. (*36*) have recently reported the crystal structure of human heme oxygenase-1. Interestingly, it is also a helical bundle with the heme binding site between two helices. The authors include a discussion of regioselectivity of the mechanism based on this structure and conclude that the specificity for the α-meso carbon site is primarily due to the steric influence of the distal helix. This is in contrast to (but not necessarily in conflict with) our generalized discussion of regiospecificity in which we conclude that electronic effects are a primary influence.

ACKNOWLEDGMENT

J.K.R. thanks Dr. Harold Bright at the ONR for supporting this work through a travel grant. We thank Prof. Alan Fersht for continued support.

REFERENCES

1. Lagarias, J. C. (1982) *Biochim. Biophys. Acta 717*, 12−19.
2. Sano, S., Sano, T., Morishima, I., Shiro, Y., and Maeda, Y. (1986) *Proc. Natl. Acad. Sci. U.S.A. 83*, 531−535.
3. Morishima, I., Fujii, H., and Shiro, Y. (1995) *Inorg. Chem. 34*, 1528−1535.
4. Gorst, C. M., Wilks, A., Yea, D. C., Ortiz de Montellano, P. R., and La Mar, G. N. (1998) *J. Am. Chem. Soc. 120*, 8875−8884.
5. Liu, Y., Moenne-Loccoz, P., Loehr, T. M., and Ortiz de Montellano, P. R. (1997) *J. Biol. Chem. 272*, 6909−6917.
6. Hernandez, G., Wilks, A., Pailesse, R., Smith, K. M., Ortiz de Montellano, P. R., and La Mar, G. N. (1994) *Biochemistry 33*, 6631−6641.
7. Takahashi, S., Ishikawa, K., Takeuchi, N., Ikeda-Saito, M., Yoshida, T., and Rousseau, D. L. (1995) *J. Am. Chem. Soc. 117*, 6002−6006.
8. Wilks, A., and Ortiz de Montellano, P. R. (1993) *J. Biol. Chem. 268*, 22357−22362.
9. Wilks, A., Torpe, J., and Ortiz de Montellano, P. R. (1994) *J. Biol. Chem. 269*, 29553−29556.
10. Torpey, J., and Ortiz de Montellano, P. R. (1996) *J. Biol. Chem. 271*, 26067−26073.
11. Torpey, J., and Ortiz de Montellano, P. R. (1997) *J. Biol. Chem. 272*, 22008−22014.
12. O'Carra, P., and Colleran, E. (1969) *FEBS Lett. 5*, 295−298.
13. Brown, S. B. (1976) *Biochem. J. 159*, 23−27.
14. Brown, S. B., Chabot, A. A., Enderby, E. A., and North, A. C. T. (1981) *Nature 289*, 93−95.
15. Hildebrand, D. P., Tang, H. L., Luo, Y. G., Hunter, C. L., Smith, M., Brayer, G. D., and Mauk, A. G. (1996) *J. Am. Chem. Soc. 118*, 12909−12915.
16. Rodriguez, J. C., Desilva, T., and Rivera, M. (1998) *Chem. Lett.*, 353−354.
17. Crusats, J., Suzuki, A., Mizutani, T., and Ogoshi, H. (1998) *J. Org. Chem. 63*, 602−607.
18. Beale, S. I. (1993) *Chem. Rev. 93*, 785−802.
19. Terry, M. J., Wahleithner, J. A., and Lagarias, J. C. (1993) *Arch. Biochem. Biophys. 306*, 1−15.
20. Lagarias, J. C. (1982) *Biochemistry 21*, 5962−5967.
21. Barker, P. D., Nerou, E. P., Cheesman, M. R., Thomson, A. J., De Oliveira, P., and Hill, H. A. O. (1996) *Biochemistry 35*, 13618−13626.
22. Barker, P. D., and Freund, S. M. V. (1996) *Biochemistry 35*, 13627−13635.
23. Thomas, P. E., Ryan, D., and Levin, W. (1976) *Anal. Biochem. 75*, 168−176.
24. Barker, P. D., Nerou, E. P., Freund, S. M. V., and Fearnley, I. M. (1995) *Biochemistry 34*, 15191−15203.
25. Wilm, M. S., and Mann, M. (1994) *Int. J. Mass Spectrom. Ion Processes 136*, 167−180.
26. Smith, K. M. (1975) *Porphyrins and Metalloporphyrins*, Elsevier, Amsterdam.
27. Antonini, E., and Brunori, M. (1971) *Hemoglobin and Myoglobin in their reactions with ligands*, North-Holland, Amsterdam.
28. Sono, M., Roach, M. P., Coulter, E. D., and Dawson, J. H. (1996) *Chem. Rev. 96*, 2841−2887.
29. Li, Y.-T., Hsieh, Y.-L., Henion, J. D., and Ganem, B. (1993) *J. Am. Soc. Mass Spectrom. 4*, 631−637.
30. Rodriguez, J. C., and Rivera, M. (1998) *Biochemistry 37*, 13082−13090.
31. Balch, A. L., Koerner, K., Latos-Grazynski, L., Lewis, J. E., St. Claire, T. N., and Zovinka, E. P. (1997) *Inorg. Chem. 36*, 3892−3897.
32. Wedemayer, G. J., Kidd, D. G., Wemmer, D. E., and Glazer, A. N. (1992) *J. Biol. Chem. 267*, 7315−7331.
33. Wagner, U. G., Müller, N., Schmitzberger, W., Falk, H., and Kratky, C. (1995) *J. Mol. Biol. 247*, 326−337.
34. Timkovich, R., and Bondoc, L. L. (1990) *Adv. Biophys. Chem. 1*, 203−247.
35. Moss, G. P. (1988) *Eur. J. Biochem. 178*, 277−328.
36. Schuller, D. J., et al. (1999) *Nat. Struct. Biol. 6*, 860−866.

BI990880Y